Subcritical convection in the presence of Soret effect within a horizontal porous enclosure heated and salted from the short sides

M. Er-Raki [(1)], M. Hasnaoui [(1)*], A. Amahmid [(1)] and M. Bourich [(2)]

[(1)] Faculty of Sciences Semlalia, Physics Department, LMFE, affiliated to CNRST (URAC, 27), Marrakesh, Morocco.

[(2)] Poly-Disciplinary Faculty, Physics Department, Safi, Morocco.

Abstract

Soret effect on double diffusive natural convection induced in a horizontal Darcy porous enclosure, saturated with a binary mixture, is studied analytically and numerically. The short vertical walls of the porous medium are subject to uniform heat and mass fluxes while its long horizontal walls are considered adiabatic and impermeable to mass transfer. The discussion is mainly focused on the specific situation for which the problem admits an equilibrium solution, possible when the buoyancy ratio N and the Soret parameter S_P are such $N = -1/(1 - S_P)$. Two solutions, characterized by the same flow rotation with different intensities, are obtained at sufficiently large values of R_T, they are termed as "stable" and "unstable". It is also demonstrated that the supercritical bifurcation of parallel flow type does not exist for this problem; only a subcritical bifurcation exists and occurs at the threshold R_{TC}^{sub}, determined analytically in terms of the governing parameters. Moreover, the existence of ranges where no parallel flow solution is possible is proved. The effect of the governing parameters on the fluid flow properties and heat and mass transfer characteristics was also examined.

Key words: Shallow horizontal enclosure, Porous medium, Binary mixture, Soret effect, Horizontal heat and mass fluxes, Analytical and numerical study, Subcritical convection.

* Corresponding author (M. Hasnaoui); E-mail address: hasnaoui@ucam.ac.ma
Tel.: +(212)-524-43-46-49; fax: +(212)-524-43-74-10.

Nomenclature

H'	height of the enclosure
L'	width of the porous layer
A_r	aspect ratio of the porous matrix, L'/H'
D	mass diffusivity of species
D_T	thermo-diffusion coefficient
g	gravitational acceleration
K	permeability of the porous medium
q'	constant heat flux per unit area
j'	constant mass flux per unit area
$\Delta T'$	characteristic temperature, $q'H'/\lambda$
$\Delta S'$	characteristic solute concentration, $j'H'/D$
Le	Lewis number, α/D
S_P	Soret parameter, $S'_0 D_T \Delta T'/(D\Delta S')$
N	buoyancy ratio, $\beta_S \Delta S'/\beta_T \Delta T'$
R_T	thermal Darcy-Rayleigh number, $g\beta_T K q' H'^2/(\lambda\alpha\nu)$
R_{TC}^{sub}	subcritical Rayleigh number
S_P^{cr}	critical value of the Soret parameter
Nu	Nusselt number
$\overline{Nu}$	mean Nusselt number
Sh	Sherwood number
$\overline{Sh}$	mean Sherwood number
T	dimensionless temperature, $(T' - T'_0)/\Delta T'$
T'_0	reference temperature
S	dimensionless solute concentration, $(S' - S'_0)/\Delta S'$
S'_0	reference solute concentration
t	dimensionless time, $t'\alpha/(H'^2\sigma)$

u	dimensionless horizontal velocity, $u = u'H'/\alpha$
v	dimensionless vertical velocity, $v = v'H'/\alpha$
x	dimensionless distance along the x-axis, $x = x'/H'$
y	dimensionless distance along the y-axis, $y = y'/H'$

Greek symbols

α	thermal diffusivity
β_S	solute concentration expansion coefficient
β_T	thermal expansion coefficient
ε	normalized porosity, ε'/σ
ε'	porosity of the porous medium
λ	thermal conductivity
ν	Kinematic viscosity of the fluid
$(\rho c)_f$	heat capacity of the fluid mixture
$(\rho c)_p$	heat capacity of the saturated porous medium
σ	heat capacity ratio, $(\rho c)_p/(\rho c)_f$
η	relaxation factor
ψ	dimensionless stream function, ψ'/α
ζ	dimensionless vorticity, $\zeta' H'^2/\alpha$

Superscript

$'$	for dimensional variable

Subscripts

$_0$	refers to a reference state
$_S$	refers to solutal
$_T$	refers to thermal

1. Introduction

Transport phenomena in porous media are of fundamental importance in many engineering applications owing to their presence and to the role that they may play in various natural, environmental and industrial processes. Diffusion counts one among the major mechanisms of transport phenomena. Oil and natural gas reservoirs exploration, safe nuclear waste underground disposal, efficient electro-chemical and metallurgical processes, and underground contaminant dispersion are some applications where these phenomena may involve. A comprehensive review of the literature concerning experimental and theoretical studies of double-diffusive natural convection in saturated porous media is documented in the recent books by Vafai (2005), Ingham and Pop (2005), Nield and Bejan (2006) and Vadasz (2008). When the molecular diffusion is generated by an imposed thermal gradient in an initially homogeneous mixture, the phenomenon is called thermodiffusion or Soret effect. The latter could be large enough to affect notably heat and mass transfer characteristics in some mixtures and it may engender specific behaviors in convective motions.

Many experimental efforts are still devoted by researchers worldwide to measure the Soret coefficient for various mixtures. For binary mixtures, this coefficient is measured as the ratio of the thermodiffusion coefficient to the molecular diffusion and the accuracy of the measurements is inevitably influenced by convection. In the review by Platten (2006), relating the different techniques used to measure the Soret coefficient, the reader learns that each technique has its own limitation, which means that the experimental approach of the phenomenon remains still a real challenge for the experimentalists. Though this realistic and alarmist conclusion of the author, outlining the difficulties inherent to the experimental approach of the phenomenon, some teams remain still involved in the experimental investigations. For instance, thermal diffusion behaviour of various binary alkane mixtures was studied in a recent paper by Blanco et al. (2008), using two different techniques (a convective method and a non-convective one). The authors concluded that the results of these two methods are in agreement in general but deviations in the order of 30 % up to 40% with data published in the literature were observed. Thermal diffusion coefficients for different binary n-alkane mixtures were studied by Yan et al. (2008) both experimentally, using the thermogravitational technique and theoretically through a remodelled nonequilibrium thermodynamic property τ. The new model proposed by the authors leads to a good agreement with their experimental data and with the data available in the literature.

Earlier, the case of a diffusion of solute generated by a temperature gradient within a horizontal layer heated from below was studied experimentally (Hurle and Jakeman, 1971; Platten and Chavepeyer, 1973) and numerically (Shteinberg, 1971; Lawson and Yang, 1973). In these pioneer works, a variety of interesting phenomena (multiple steady/oscillatory states, subcritical flows, standing/travelling waves and Hopf's bifurcations are some examples of these phenomena), engendered by the nature of coupling between thermosolutal convection and thermodiffusion were reported and discussed. Later, Soret convection in a binary fluid mixture was investigated by Knobloch and Moore (1988) for different thermal boundary conditions using normal ^3He-^4He and ethanol-water mixtures. By means of a stability analysis, the thresholds for the onset of stationary and oscillatory convection were predicted for different thermal boundary conditions. The Soret effect in an initially homogeneous ternary mixture of water-ethanol-isopropanol, heated from below, was investigated by Larre et al. (1997). The discrepancy observed between the experimental critical parameters for the onset of convection and theoretical predictions was recovered when the cross-diffusional effects were incorporated in the linear stability analysis. In the presence of Soret effect, criteria for the onset of motion via a stationary convection, Hopf's bifurcation and oscillatory convection in an infinite porous layer saturated with a binary fluid were derived by Sovran et al. (2001) on the basis of the stability analysis. The critical Rayleigh numbers, characterizing the onset of supercritical and subcritical convection, were predicted analytically in terms of the governing parameters of the problem by Delahaye et al. (2002) while studying the influence of Soret effect on natural convection in a binary horizontal fluid layer heated from below and having a non-deformable free upper surface. Soret driven thermosolutal convection in a shallow horizontal Brinkman porous enclosure, with a stress-free upper surface and heated from below was studied analytically and numerically by Er-Raki et al. (2005). It was found that, depending on the sign of the separation parameter, the Soret effect can play a stabilizing or a destabilizing role. The onset of convection and finite amplitude flow due to Soret effect within a horizontal sparsely packed porous enclosure heated from below was studied by Bourich et al. (2005). The thresholds for the onset of stationary and finite amplitude convection were determined analytically as function of the governing parameters while the threshold for the Hopf's bifurcation was obtained on the basis of the linear stability analysis. Soret-driven convection in a porous cavity saturated with a binary fluid and heated from above or below was studied analytically and numerically by Charrier-Mojtabi et al. (2007). Using the linear stability analysis, the authors found that the equilibrium solution loses its stability via a stationary bifurcation or a Hopf's bifurcation, depending on the separation ratio and the normalized porosity of the medium. The Soret effect on thermo-convection in a horizontal infinite layer of binary liquid mixtures with weak concentration diffusivity and large separation numbers was studied by Ryskin et al. (2003). They worked with a separation ratio varying in the range [0, 100]. Their results showed that both linear and nonlinear convective behaviours were significantly altered by the concentration field as compared to single-component systems. Charrier-Mojtabi et al. (2004) investigated the Soret effect under the simultaneous actions of vibrational and gravitational accelerations in a porous cavity saturated by a binary mixture. They founded that, when the direction of vibration is considered parallel to the temperature gradient, vibration has a stabilizing effect for both the stationary and the Hopf's bifurcations; the action of vibration reduces the number of convective rolls and the Hopf's frequency. However, when the direction of vibration is perpendicular to the temperature gradient, the effect of vibration becomes destabilizing.

In the references cited above, the studied configurations were assumed impermeable to mass transfer. In comparison, few investigations have considered Soret effect within permeable horizontal systems. Hence, in a fluid saturated porous layer with horizontal boundaries maintained at constant but different temperatures and solute concentrations, Alex and Patil (2001) used the Galerkin technique to study the effect of the gravity gradient on the onset of thermosolutal convection due to thermal diffusion. The results presented showed that the Soret parameter affects the convective pattern only when its magnitude is large enough both in the presence and the absence of the gravity field variations. Thermosolutal convection combined with Soret effect in a binary fluid saturating a shallow horizontal porous layer subjected to cross fluxes of heat and mass was studied by Bennacer et al. (2003). The existence of both natural and anti-natural flows in the presence of a vertical destabilizing concentration gradient was reported in this study. The Soret effect on thermosolutal convection induced in a horizontal Darcy porous layer subject to constant heat and mass fluxes was considered by Bourich et al. (2004a). The thresholds for the onset of supercritical and subcritical convection were predicted explicitly as functions of the governing parameters and it is demonstrated that there exist combinations of the governing parameters for which the Soret effect imposes a reversal of the concentration gradient in the horizontal direction. In a recent investigation, combined effects of thermodiffusion and lateral heating on double diffusive natural convection within a horizontal porous layer, saturated with a binary fluid and subjected to uniform fluxes of heat and mass on its long sides, were studied analytically and numerically by Mansour et al. (2008). The short sides of the layer are impermeable to mass transfer and exposed to a perturbating constant heat flux. Five different regions, describing different flow behaviors, were delineated in the M*-Le plane and their locations depends on the lateral heating. The effect of the latter is found to be considerable on the flow and heat transfer but remains negligible on the mass transfer.

The main objective of the present investigation consists to study analytically and numerically the Soret effect on double diffusive natural convection induced in a horizontal Darcy porous layer subject to lateral heat and mass fluxes. This problem is classified in the category of problems where heat and mass gradients are imposed horizontally. In the absence of Soret effect, an equilibrium solution is possible when thermal and solutal buoyancy forces are opposing each other. In previous works, the onset of the convective regime in vertical layers for the particular situation where the buoyancy forces are opposing and of equal intensity was studied both in fluid medium by Gobin and Bennacer (1994) and Ghorayeb and Mojtabi (1997) and in porous medium by Mamou et al. (1998) and later by Mamou (2002). The number of papers treating the problem with experimental boundary conditions and taking into account the flow configuration confinement is very small, though different thermal and solutal boundary conditions have been considered to investigate the thermal diffusion phenomena. In practical situations, the temperature usually varies along the heated or cooled walls. In fact, in laboratory, the temperature of the boundaries in a convection experiment can be fixed only when the Nusselt number is much lower than the ratio of conductivities between the plates and the fluid (see for instance Otero et al., 2002). Therefore, for high Nusselt number, constant heat flux boundary conditions are a more appropriate approach to study convective phenomena relating to many industrial or natural problems.

The present work focuses on the particular situation where $N = 1/(S_P - 1)$. The effect of the governing parameters on the fluid flow properties and heat and mass transfer characteristics is examined and the resulting sub-critical bifurcations are identified.

2. Problem formulation

The physical problem under study is sketched in Fig. 1. The configuration is a two-dimensional horizontal shallow porous layer of height H' and width L' filled with a binary mixture. The short vertical walls of the layer are subject to uniform fluxes of heat, q', and mass, j', while its horizontal long walls are considered adiabatic and impermeable to mass transfer. The porous matrix is assumed isotropic and homogeneous and the Darcy law is adopted. The diluted binary solution that saturates the porous medium is modeled as a Boussinesq incompressible fluid for which the fluid density varies according to the relationship given by:

$$\rho = \rho_0 \left[1 - \beta_T (T' - T'_0) - \beta_S (S' - S'_0)\right]$$

The subscript "0" refers to a reference state.

Using the vorticity-stream function formulation, the dimensionless steady equations governing the Darcy model in the presence of Soret effect are as follows:

$$\zeta = R_T \left(\frac{\partial T}{\partial x} + N \frac{\partial S}{\partial x} \right) \tag{1}$$

$$u \frac{\partial T}{\partial x} + v \frac{\partial T}{\partial y} = \nabla^2 T \tag{2}$$

$$u \frac{\partial S}{\partial x} + v \frac{\partial S}{\partial y} = \frac{1}{Le} \left(\nabla^2 S + S_P \nabla^2 T \right) \tag{3}$$

$$\nabla^2 \psi = -\zeta \tag{4}$$

$$u = \frac{\partial \psi}{\partial y} \qquad ; \qquad v = -\frac{\partial \psi}{\partial x} \tag{5}$$

The associated boundary conditions are given by:

$$\left.\begin{array}{llll} x = \pm A_r/2 & \psi = 0, & \dfrac{\partial T}{\partial x} = 1, & \dfrac{\partial S}{\partial x} = 1 - S_P \\ y = \pm 1/2 & \psi = 0, & \dfrac{\partial T}{\partial y} = 0, & \dfrac{\partial S}{\partial y} = 0 \end{array}\right\} \tag{6}$$

where u, v, ζ, ψ, T and S represent respectively the dimensionless horizontal and vertical components of the velocity, vorticity, stream function, temperature and concentration.

The system of equations presented above shows that the present problem is governed by four dimensionless parameters which are the thermal Rayleigh number, R_T; the Lewis number, Le; the Soret parameter, S_P; and the solutal to thermal buoyancy ratio, N. They describe respectively the thermal driving force, the relative importance of the thermal diffusivity with respect to the solute one, the thermo-diffusion phenomenon (Soret effect) and the importance of solutal buoyancy forces due to the applied mass flux, j'.

The local Nusselt and Sherwood numbers, characterizing respectively the local heat and mass transfers through the layer, are defined as follows:

$$Nu(y) = A_r / \Delta T(y) = 1/(\Delta T(y)/A_r) \quad \text{and} \quad Sh(y) = A_r / \Delta S(y) = 1/(\Delta S(y)/A_r) \qquad (7)$$

where $\Delta T(y) = T(A_r/2, y) - T(-A_r/2, y)$ and $\Delta S(y) = S(A_r/2, y) - S(-A_r/2, y)$ are the side to side dimensionless local temperature and concentration differences, respectively.

It should be noted that the above definitions of Nu and Sh (based on the temperature and concentration calculated on the side walls) does not allow a comparison with the analytical solution (described hereafter) and are not valid in the vicinity of the side walls due to the returning flow (see for instance Lamsaadi et al., 2006). Therefore, the Nusselt and Sherwood numbers must be calculated using temperature and concentration differences between two contiguous vertical sections in the central part of the enclosure to avoid the effect of the end sides. Thus, by considering two infinitesimally close sections around the plane x = 0, and by analogy with Eq. (7), the local Nusselt and Sherwood numbers can be defined as follows:

$$Nu(y) = \lim_{\delta x \to 0} \delta x / \delta T(y) = \lim_{\delta x \to 0} 1/(\delta T(y)/\delta x) = 1/(\partial T/\partial x)_{x=0} \qquad (8)$$

$$Sh(y) = \lim_{\delta x \to 0} \delta x / \delta S(y) = \lim_{\delta x \to 0} 1/(\delta S(y)/\delta x) = 1/(\partial S/\partial x)_{x=0} \qquad (9)$$

where δx is the distance between these sections.

Then, the mean Nusselt and Sherwood numbers at different locations are calculated by the expressions:

$$\overline{Nu} = \int_{-1/2}^{1/2} Nu(y)\,dy \qquad \text{and} \qquad \overline{Sh} = \int_{-1/2}^{1/2} Sh(y)\,dy \tag{10}$$

These expressions of Nusselt and Sherwood numbers are used in the numerical calculations to avoid the effect of the end regions where the analytical solution is not valid. In order to show the non validity of the expressions of Nu and Sh given by Eq. (7), comparative results with the analytical solution will be presented hereafter.

3. Numerical method

The governing equations (1) to (3) were solved in their transient form using a second-order finite difference schemes and the iterative procedure was performed by using the Alternate Direction Implicit method **(ADI)**. The stream function field was obtained from Eq. (4) using the point successive-over-relaxation method **(PSOR)**. The numerical results reported in this paper were performed with a non uniform grid (finer grid near the confining walls to capture flow details near the boundaries) of 201×81 and an aspect ratio A_r varying in the range $4 \le A_r \le 12$.

Note that the present study is concerned only with the steady-state regime but the equations were solved in their transient form until the establishment of the stationary state. In Eq. (1), the transient term $(\eta \frac{\partial \xi}{\partial t})$ contains the relaxation factor η. Preliminary tests concerning the effect of η have shown that an appropriate choice of the value of this parameter in the range $0.01 \le \eta \le 10$ could lead to a considerable reduction of the computation time. More details concerning the validation of the numerical code are given in the references by Amahmid et al. (1999) and Bourich et al. (2004b).

Typical numerical results, in terms of streamlines (a), isotherms (b) and iso-concentrations (c), are presented in Fig. 2 for $A_r = 12$, $R_T = 500$, Le = 3, $S_P = 2$ and N = 1. It can be seen from this figure that the flow in the core region of the enclosure is parallel to the horizontal walls (long sides) and the temperature and concentration fields are linearly stratified in the horizontal direction even if the active boundaries of the cavity are the short ones. These observations, which are at the origin of the analytical solution proposed in this study (solution valid far from the vertical walls where the side-effects are important), have been exploited by several authors in the past.

4. Analytical solution

In general, it is not possible to perform an exact analytical solution for the set of equations (1) to (3) whatever are the imposed boundary conditions. However, in the case of shallow enclosures (A_r>>1), an approximate analytical solution can be developed in the central part of the cavity on the basis of the following approximations:

$$\psi(x,y) \cong \psi(y), \qquad T(x,y) \cong C_T x + \theta_T(y) \qquad \text{and} \qquad S(x,y) \cong C_S x + \theta_S(y) \tag{11}$$

where C_T and C_S are respectively unknown constant temperature and concentration gradients in the horizontal direction.

Note that the parallel flow assumption has been used earlier by Cormack et al. (1974) while studying natural convection in a shallow cavity with differentially heated end walls and later by many other authors. This assumption was also used more recently to study double diffusion convection without (Amahmid et al., 2000) and with (Bourich et al., 2004c) Soret effect.

Taking these approximations into account, the steady form of the governing equations (1) to (3) can be reduced to the following set of ordinary differential equations:

$$\frac{d^2\psi}{dy^2} = -R_T\left(C_T + NC_S\right) \tag{12}$$

$$\frac{d^2\theta_T}{dy^2} = C_T \frac{d\psi}{dy} \tag{13}$$

$$\frac{d^2\theta_S}{dy^2}+S_P\frac{d^2\theta_T}{dy^2}=LeC_S\frac{d\psi}{dy} \tag{14}$$

The analytical resolution of the set of ordinary differential equations (12) to (14) with consideration of the associated boundary conditions (6), leads to the following solution:

$$\psi(y)=\psi_0\left(-4y^2+1\right) \tag{15}$$

$$T(x,y)=C_T x+\psi_0 C_T\left(\frac{-4}{3}y^3+y\right) \tag{16}$$

$$S(x,y)=C_S x+\psi_0\left(C_S Le-C_T S_P\right)\left(\frac{-4}{3}y^3+y\right) \tag{17}$$

where ψ_0 is the stream function at the centre of the enclosure; it is defined by the following expression:

$$\psi_0=\frac{R_T}{8}\left(C_T+NC_S\right) \tag{18}$$

The constants C_T and C_S were determined by performing global balances of energy and solute transfer across any transversal section of the enclosure (Trevisan and Bejan, 1986). These balances lead to the following integrals:

$$\int_{-1/2}^{1/2}(uT-\frac{\partial T}{\partial x})dy=-1 \tag{19}$$

$$\int_{-1/2}^{1/2}[uS-\frac{1}{Le}(\frac{\partial S}{\partial x}+S_P\frac{\partial T}{\partial x})]dy=\frac{-1}{Le} \tag{20}$$

Then, the temperature and concentration horizontal gradients C_T and C_S are deduced as follows:

$$C_T=\frac{1}{1+8\psi_0^2/15} \tag{21}$$

$$C_S=\frac{1}{1+8Le^2\psi_0^2/15}-S_P\frac{(1-8Le\psi_0^2/15)}{(1+8Le^2\psi_0^2/15)(1+8\psi_0^2/15)} \tag{22}$$

According to the equations (8), (9) and (10), the local Nusselt and Sherwood numbers are found to be constant, they are given by:

$$Nu = \overline{Nu} = \frac{1}{C_T} = 1 + 8\psi_0^2 / 15 \tag{23}$$

$$Sh = \overline{Sh} = \frac{1}{C_S} = \frac{(1 + 8Le^2\psi_0^2 / 15)(1 + 8\psi_0^2 / 15)}{(1 + 8\psi_0^2 / 15) - S_P(1 - 8Le\psi_0^2 / 15)} \tag{24}$$

This implies that both Eqs. (8-9) and (10) can be used to evaluate analytically the Nusselt and Sherwood numbers. Numerically, Nu and Sh deduced from Eq. (7) disagree with the analytical solution due to the edge effects. To illustrate this disagreement, we present in Fig. 3 the variations of the temperature and concentration gradients ($\partial T/\partial x$ and $\partial S/\partial x$) at mid-height of the enclosure (y = 0) for $R_T = 500$, Le = 3, $S_P = 2$, N = 1 and $A_r = 12$. It appears clearly from this figure that the analytical and numerical results are in good agreement in the core region. However, the disagreement is considerable near the vertical walls where the analytical solution is not valid.

Note that all the unknown parameters appearing in the solution given by Eqs. (15)-(17) are depending on ψ_0. An equation for the latter can be established by combining Eqs. (18), (21) and (22), which leads to the following polynomial of 5th order:

$$A\psi_0^5 + B\psi_0^3 - C\psi_0^2 + D\psi_0 - E = 0 \tag{25}$$

where A, B, C, D and E are expressed as:

$$\begin{cases} A = 512Le^2 \\ B = 960(Le^2 + 1) \\ C = 120R_T(Le^2 + NS_PLe + N) \\ D = 1800 \\ E = 225R_T(1 - NS_P + N) \end{cases}$$

The present study focuses on the particular situation corresponding to $E = 0$; relation satisfied if $N = -1/(1 - S_P)$. In the absence of the Soret effect, this case corresponds to N = -1 for which the buoyancy forces induced by the thermal and solutal effects opposite each other and have the same intensity.

By setting $E = 0$, Eq. (25) reduces to:

$$A\psi_0^4 + B\psi_0^2 - C\psi_0 + D = 0 \tag{26}$$

For a given set of the governing parameters R_T, Le, S_P and N, the fourth order polynomial of Eq. (26) is solved numerically using the bisection method. Owing to the relation $N = -1/(1 - S_P)$ between N and S_P, the present problem is governed only by three parameters which are R_T, Le and S_P.

5. Results and discussion

Mathematical analysis of Eq. (26) shows that the latter has only two solutions (when they exist). At large R_T (R_T>>1), these solutions are given by:

$$\psi_0 \approx \sqrt[3]{\frac{120\left(Le^2 + (S_P Le + 1)/(S_P - 1)\right)}{A}} R_T^{1/3} \tag{27}$$

and

$$\psi_0 \approx \frac{D}{120\left(Le^2 + (S_P Le + 1)/(S_P - 1)\right)} R_T^{-1} \tag{28}$$

Eqs. (27) and (28) indicate that ψ_0 varies as $R_T^{1/3}$ and R_T^{-1} and the corresponding flows rotate in the same direction. In fact, as the parameters A, B and D are positive, Eq. (26) indicates that $C\psi_0 > 0$, which means that ψ_0 and C have the same sign, then:

$$\psi_0 < 0 \qquad \text{for} \qquad 1 - \frac{1}{Le} < S_P < 1 \tag{29}$$

and

$$\psi_0 > 0 \qquad \text{for} \qquad S_P > 1 \quad \text{or} \quad S_P < 1 - \frac{1}{Le} \tag{30}$$

On the basis of this discussion, it can be noted that the S_P-Le plane can be divided into two regions I and II delineated in Fig. 4 and characterized by counter-clockwise and clockwise flows, respectively. The thermodiffusion effect on the flow rotation is clearly shown in this figure. Hence, in the absence of Soret effect ($S_P = 0$), the flow is clockwise for $Le < 1$ and counter-clockwise for $Le > 1$. In the presence of Soret effect, only counter-clockwise flows are possible for $S_P > 1$ regardless of the value assigned to Le. However, for $S_P < 1$, the flow is clockwise for $Le < \dfrac{1}{1 - S_P}$ and counter-clockwise for $Le > \dfrac{1}{1 - S_P}$.

It is well known that, when the convective flow bifurcates from the rest state through zero amplitude convection $(\psi_0 = 0)$, the bifurcation is qualified as a supercritical. In the contrary, when the bifurcation occurs through finite amplitude convection $(\psi_0 \neq 0)$, the bifurcation is known as a sub-critical. Now, let us focus the attention on the bifurcations possible for this problem through Eq. (26). By examining this equation, it appears that no supercritical bifurcation is possible; only a subcritical bifurcation exists and the latter occurs at $R_T = R_{TC}^{sub}$ given by:

$$R_{TC}^{sub} = \frac{\tilde{\psi}_0 \left(4A\tilde{\psi}_0^2 + 2B\right)}{120\left|Le^2 + (S_P Le + 1)/(S_P - 1)\right|} \qquad (31)$$

where: $\tilde{\psi}_0 = \sqrt{\left(\dfrac{-B + \sqrt{\Delta}}{6A}\right)}$ with $\Delta = B^2 + 12AD$

The variations of R_{TC}^{sub} with S_P are illustrated in Fig. 5 for Le = 3 and 10. It can be seen from this figure that R_{TC}^{sub} increases by increasing S_P in the ranges $S_P < 1 - 1/Le$ and $S_P > 1$. However, the tendency is inverted in the range $1 - 1/Le < S_P < 1$ where R_{TC}^{sub} undergoes a very fast decrease with S_P. Also, it can be seen that R_{TC}^{sub} tends towards 0 and infinity respectively when S_P approaches 1 and $(1 - 1/Le)$. This indicates the absence of the parallel flow solution for $S_P \cong 1 - 1/Le$ and convection starts at $R_T \cong 0$ for $S_P \cong 1$. Note that, at sufficiently large values of $|S_P|$, R_{TC}^{sub} tends towards an asymptotic limit given by:

$$R_{TC}^{sub} = \frac{\tilde{\psi}_0\left(4A\tilde{\psi}_0^2 + 2B\right)}{120\left(Le^2 + Le\right)} \tag{32}$$

The effect of the thermal Rayleigh number, R_T, on the fluid flow and heat and mass characteristics is illustrated in Fig. 6 in terms of ψ_0 (a), Nu (b) and Sh^{-1} (c-d) variations with R_T for (Le, S_P) = (10, 3) and (10, 0.92). The combinations of Le and S_P are chosen so that both clockwise and counter clockwise flows can be observed. The mass transfer is characterised by Sh^{-1} (i.e. the inverse of the Sherwood number) in order to avoid the singularities observed on the curves of Sh when the horizontal gradient of concentration is zero (which yield infinite Sh). Bearing in mind the definitions of supercritical and sub-critical bifurcations, a global examination of Fig. 6 could lead to a wrong deduction concerning the nature of the bifurcations observed in this figure. In fact, due to the weak values of ψ_0 at the onset of convection [$|\psi_0| \approx 0.134$ for (Le, S_P) = (10, 3) and (10, 0.92)], resulting from the relatively high value of Le (Le = 10), one might think wrongly that the bifurcation is super-critical. However, this ambiguity is lifted by a close inspection via the zoom which indicates clearly that the bifurcation is of sub-critical nature. By choosing a lower value of Le (Le = 1), we found that the amplitude corresponding to the onset of convection is relatively important (of order of unity) and the nature of bifurcation is clearly of sub-critical aspect (results not presented). In Fig. 6, the onset of the subcritical convection occurs at the critical Rayleigh number R_{TC}^{sub} = 1.915 and 8.045 respectively for (Le, S_P) = (10, 3) and (10, 0.92). Therefore $R_{TC}^{sub}(S_P = 0.92) > R_{TC}^{sub}(S_P = 3)$, which is in accordance with the results of Fig. 5 illustrating the variations of R_{TC}^{sub} with S_P. It can be seen from Fig. 6 that only one of the two analytical solutions is validated numerically; it is termed as a "stable" solution. The other solution could not be validated numerically and it is termed as "unstable". Figs. 6(a) and 6(b), show that $|\psi_0|$ and Nu corresponding to the stable branches increase with R_T. Analytically, Nu varies as

$R_T^{2/3}$ at large R_T. For the unstable branches, these quantities are nearly constant and close to 0 and 1 respectively (i.e. values of the purely diffusive regime). The variations of Sh^{-1} with R_T, presented in Figs. 6c-d, show that the curves corresponding to the "stable" solutions exhibit different tendencies and Sh^{-1} approaches zero at large R_T (analytically Sh^{-1} varies as $R_T^{-2/3}$). The "unstable" branch corresponding to Sh^{-1} remains close to the value of the purely diffusive regime ($Sh^{-1} \cong 1 - S_P$). For the combination (Le, S_P) = (10, 3), Fig 6(c) shows that there exists a critical value of R_T ($R_T^0 \cong 2.96195$) for which Sh^{-1} = 0, which means that the horizontal gradient of concentration is zero. Beyond this value of R_T, a change in the sign of the horizontal gradient of concentration is observed ($Sh < 0$ for $R_{TC}^{sub} < R_T < R_T^0$ and $Sh > 0$ for $R_T > R_T^0$). The iso-concentration contours presented in Figs. 7 for R_T = 2.5, 2.96195 and 3.5 show a vertical stratification of the concentration for $R_T = R_T^0$ and different stratification tendencies for the other values of R_T surrounding R_T^0. The concentration profiles at mid-height (Fig. 7(d)) and mid-width (Fig. 7(e)) of the enclosure confirm these deductions and indicate that the vertical profile of concentration obtained for $R_T = R_T^0$ is not linear.

The Soret effect is illustrated by presenting in Figs. 8(a)-(c) the evolutions of ψ_0, Nu and Sh with S_P for Le = 3 and R_T = 100. The range [-4, 4] corresponding to the variation of S_P is selected to include both critical values of S_P previously mentioned; 1-1/Le (0.666 for this case) and 1, in the vicinity of which the fluid flow and heat and mass transfers magnitudes undergo important changes. Also, in this range of S_P, a change in the flow direction occurs (i.e. a change in the sign of ψ_0). Fig.8a shows that the flow is counter-clockwise for $S_P \le S_P^{cr1}$ and $S_P > 1$ and clockwise for S_P varying in the range $S_P^{cr2} \le S_P < 1$, while there is no parallel flow solution in the range $S_P^{cr1} \le S_P < S_P^{cr2}$ ($S_P^{cr1} = 0.6454$ and $S_P^{cr2} = 0.6856$). At first glance, Figs. 8a-c show that the quantities $|\psi_0|$, Nu and Sh corresponding to the stable branches vary qualitatively in the same way. More precisely, they decrease with S_P for both $S_P \le S_P^{cr1}$ and $S_P > 1$ by exhibiting asymptotic evolutions at large $|S_P|$ and increase with this parameter in the range $S_P^{cr2} \le S_P < 1$. When S_P approaches 1 (i.e. $N \to \infty$), it can be observed that all these quantities tend towards infinite values; limit in accordance with Eqs. (27), (23) and (24). Taking into account the fact that $\psi_0 \to \infty$ when S_P tends towards 1, it can be deduced from Eqs. (16), (17), (21) and (22) that both the horizontal and vertical gradients of the temperature and concentration are nearly zero within the enclosure. This implies that, in the vicinity of this particular value of S_P, uniform temperature and concentration fields are generated in the cavity. On the other hand and as a particular behaviour observed in the evolution of Sh, the horizontal gradient of concentration is also 0 ($Sh \to \infty$) for another value of S_P ($S_P \cong - 0.47$) far from $S_P = 1$ as shown in Fig. 8c; this case corresponds analytically to $C_S = 0$. Finally, for the unstable branch, ψ_0 remains near 0 (rest state) by varying S_P in its range. Then the heat and mass transfers are dominated by the diffusive regime ($Nu \cong 1$ and $Sh \cong 1/ (1-S_P)$).

6. Conclusion

Fluid flows and heat and mass transfers induced by natural convection combined with Soret effect are studied analytically and numerically in a horizontal porous layer submitted, on its vertical short sides, to uniform heat and mass fluxes. The study focuses on the particular situation where the solutal to thermal buoyancy forces ratio is related to the Soret parameter by the relation $N = -1/(1 - S_P)$ for which the rest state is a solution of the problem. Only the sub-critical convection was found possible for this case and its threshold was determined analytically versus the governing parameters. It is also shown that the S_P-Le plane can be divided into two parallel flow regions; in one region the flow is counter-clockwise and it is clockwise in the other. At sufficiently large values of R_T, it is demonstrated that the fourth order equation of ψ_0 has two solutions termed as "stable" and "unstable" and varying respectively as $R_T^{1/3}$ and R_T^{-1}. The flows corresponding to these solutions are rotating in the same direction with different intensities. Finally, it is found that for $S_P \cong 1 - 1/Le$, the critical Rayleigh number for the onset of sub-critical convection becomes infinite which means that no parallel flow solution is possible for this case.

References:

Amahmid, A., Hasnaoui, M., Vasseur, P. (1999). "Etude analytique et numérique de la convection naturelle dans une couche poreuse de Brinkman doublement diffusive". *Int. J. Heat Mass Transfer,* Vol. 42, pp. 2991–3005.

Alex, S.M. and Patil, P.R. (2001), "Effect of variable gravity field on Soret driven thermosolutal convection in a porous medium", *Int. Comm. Heat Mass Transfer*, Vol. 28, pp. 509-518.

Amahmid, A., Hasnaoui, M., Mamou, M. and Vasseur, P. (2000), "On the transition between aiding and opposing double diffusive flows in a vertical porous matrix", *J. Porous Media*, Vol. 3, pp. 123-137.

Bennacer, R., Mahidjiba, A., Vasseur, P., Beji, H. and Duval, R. (2003), "The Soret effect on convection in a horizontal porous domain under cross temperature and concentration gradients", *Int. J. Numer. Meth. Heat Fluid Flow*, Vol. 13, pp. 199–215.

Blanco, P., Polyakov, P., Bou-Ali, M. and Wiegand, S. (2008), "Thermal diffusion values for some alkane mixtures: a comparison between thermogravitational column and thermal diffusion forced Rayleigh scattering", *J. Phys. Chem. B*, Vol. 112, pp. 8340-8345.

Bourich, M., Hasnaoui, M., Amahmid, A. and Mamou, M. (2004a), "Soret convection in a shallow porous cavity submitted to uniform fluxes of heat and mass", *Int. Comm. Heat Mass Transfer*, Vol. 31, pp. 773-782.

Bourich, M., Hasnaoui, M. and Amahmid, A. (2004b), "Double-diffusive natural convection in a porous enclosure partially heated from below and differentially salted", *Int. J. Heat Fluid Flow*, Vol. 25, pp. 1034-1046.

Bourich, M., Hasnaoui, M., Mamou, M. and Amahmid, A. (2004c), "Soret effect inducing Subcritical and Hopf bifurcations in a shallow enclosure filled with a clear binary fluid or a saturated porous medium: A comparative study", *Phys. Fluids*, Vol. 16, pp. 551-568.

Bourich, M., Hasnaoui, M., Amahmid, A. and Mamou, M. (2005), "Onset of convection and finite amplitude flow due to Soret effect within a horizontal sparsely packed porous enclosure heated from below", *Int. J. Heat Fluid Flow*, Vol. 26, pp. 513-525.

Charrier-Mojtabi, M.C., Elhajjar, B. and Mojtabi, A. (2007), "Analytical and numerical stability analysis of Soret-driven convection in a horizontal porous layer", *Phys. Fluids*, Vol. 19, 124104.

Charrier-Mojtabi, M.C., Razi, Y.P., Maliwan, K., Mojtabi, A. (2004), "Influence of vibration on Soret-driven convection in porous media", *Numerical Heat Transfer*, *Part A,* Vol. 46, pp. 981–993.

Cormack, D.E., Leal, L.G. and Imberger, J. (1974), "Natural convection in a shallow cavity with differentially heated end walls, Part 1: Asymptotic Theory", *J. Fluid Mechanics*, Vol. 65, pp. 209-230.

Delahaye, R., Bahloul, A. and Vasseur, P. (2002), "Influence of the Soret effect on convection in a binary fluid layer with a free upper surface", *Int. Comm. Heat Mass Transfer*, Vol. 29, pp. 433-442.

Er-Raki, M., Hasnaoui, M., Amahmid, A. and Bourich, M. (2005), "Soret driven thermosolutal convection in a shallow porous layer with a stress-free upper surface", *Engineering Computations*, Vol. 22, pp. 186-205.

Ghorayeb, K. and Mojtabi, A. (1997), "Double diffusive convection in a vertical rectangular cavity", *Phys. Fluids*, Vol. 9, no 8, pp. 2339-2348.

Gobin, G. and Bennacer R. (1994). "Double diffusion in a vertical fluid layer: onset of the convective regime", *Phys. Fluids*, Vol.6, no 1, pp. 59-67.

Hurle, D.T. and Jakeman, E. (1971), "Soret-driven thermosolutal convection", *J. Fluid Mech.*, Vol. 47, pp. 667-687.

Ingham, D.B. and Pop I. (eds.) (2005), "Transport phenomena in porous media III", Elsevier, Oxford.

Knobloch, E. and Moore, D.R. (1988), "Linear stability of experimental Soret convection", *Physical Review A*, Vol. 37, pp. 860-870.

Lamsaadi, M., Naïmi, M. and Hasnaoui, M. (2006), "Natural convection heat transfer in shallow horizontal rectangular enclosures uniformly heated from the side and filled with non-Newtonian power law fluids", *Energy Conversion and Management*, Vol. 47, pp. 2535-2551.

Larre, J.P., Platten, J.K. and Chavepeyer, G. (1997), "Soret effects in ternary systems heated from below", *Int. J. Heat Mass Transfer*, Vol. 40, pp. 545-555.

Lawson, M.L. and Yang, W.J. (1973), "The stability of a layer of binary gas mixture heated from below", *J. Fluid Mech.*, Vol. 57, pp. 103-110.

Mamou, M. (2002). “Stability analysis of thermosolutal convection in a vertical packed porous enclosure”, *Phys. Fluids*, Vol. 14, pp. 4302-4314.

Mamou, M., Hasnaoui, M., Amahmid, A. and Vasseur, P. (1998). “Stability analysis of double-diffusive convection in a vertical Brinkman porous enclosure”, *Int. Comm. Heat Mass Transfer*, Vol. 25, pp. 491-500.

Mansour, A., Amahmid, A. and Hasnaoui, M. (2008), “Soret effect on thermosolutal convection developed in a horizontal shallow porous layer salted from below and subject to cross fluxes of heat”, *Int. J. Heat Fluid Flow*, Vol. 29, pp. 306-314.

Nield, D.A. and Bejan, A. (2006). “Convection in Porous Media (3rd ed.)”, Springer, New York.

Otero, J., Wittenberg, R.W., Worthing, R.A. and Doering, C.R. (2002), **“**Bounds on Rayleigh–Bénard convection with an imposed heat flux”, *J. Fluid Mech*, Vol.. 473, pp. 191-199.

Platten, J.K. and Chavepeyer, G. (1973), “Oscillatory motion in Bénard cell due to the Soret effect”, *J. Fluid Mech.*, Vol. 60, pp. 305-319.

Platten, J.K. (2006), “The Soret effect: A Review of Recent Experimental Results”, *J. Applied Mechanics*, Vol. 73, pp. 5-15.

Ryskin, A., Müller, H.W., Pleiner, H. (2003), **“**Thermal convection in binary fluid mixtures with a weak concentration diffusivity, but strong solutal buoyancy forces**”,** *Phys. Rev.*, E, Vol. 67, pp. 046302.1-046302.8.

Shteinberg, V.A. (1971), “Convective instability of a binary mixture particularly in the neighborhood of the critical point”, *J. App. Math. Mech,* Vol. 35, pp. 335-345.

Sovran, O., Charrier-Mojtabi, M.C. and Mojtabi, A. (2001), “Naissance de la convection thermo-solutale en couche poreuse infinie avec effet Soret”, *C. R. Acad. Sci. Paris*, Vol. 329, pp. 287-293.

Trevisan, O.V. and Bejan, A. (1986), “Mass and heat transfer by natural convection in a vertical slot filled with porous medium”, *Int. J. Heat Mass Transfer*, Vol. 29, pp. 403–415.

Vadasz, P. (ed.) (2008). “Emerging Topics in Heat and Mass Transfer in Porous Media”, Springer, New York.

Vafai K. (ed.) (2005). “Handbook of Porous Media (2nd ed.)”, Taylor & Francis, New York.

Yan, Y., Blanco, P., Saghir, M.Z. and Bou-Ali, M. (2008), “An improved theoretical model for thermal diffusion coefficient in liquid hydrocarbon mixtures: comparison between experimental and numerical results”, *J. Chem. Phys.*, Vol. 129, 194507.

List of figures

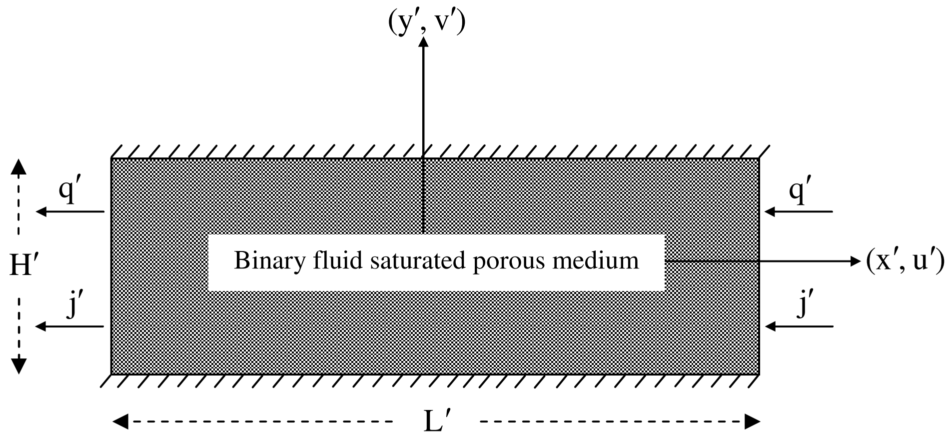

Fig. 1 (Er-Raki et al.)

($\psi_{max} = 5.85$, $\psi_{min} = 0$)

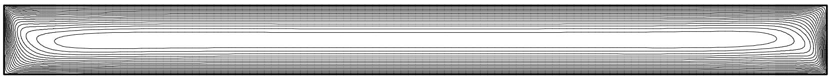

($T_{max} = 0.579$, $T_{min} = -0.581$)

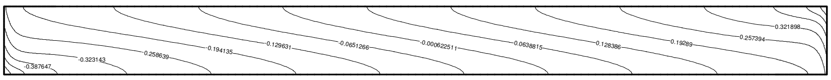

($S_{max} = 0.29$, $S_{min} = -0.29$)

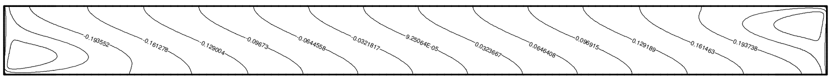

Fig. 2 (Er-Raki et al.)

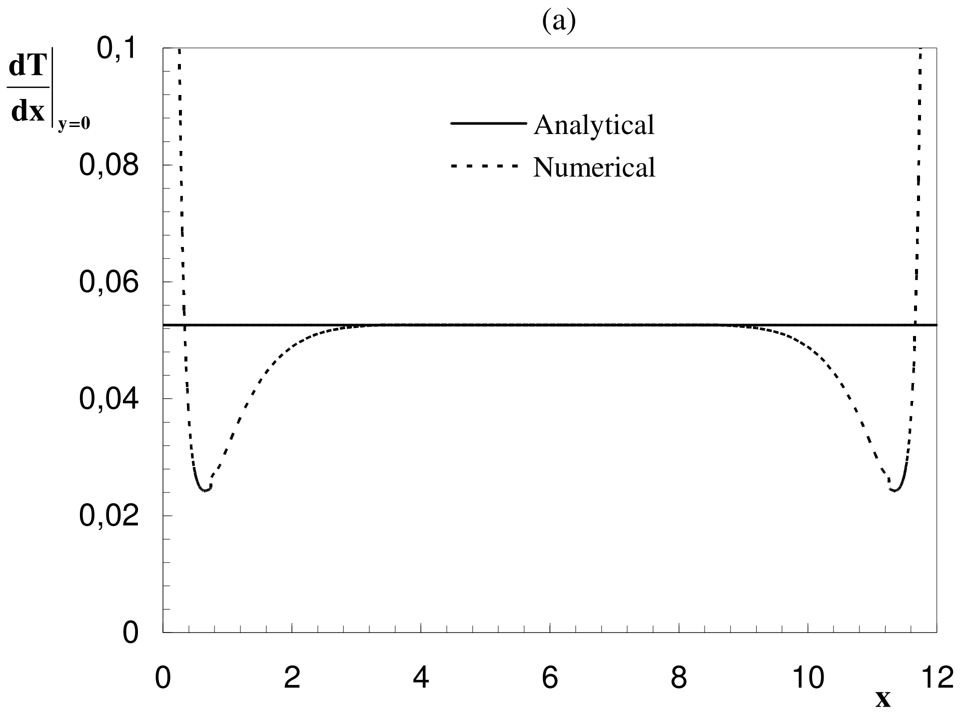

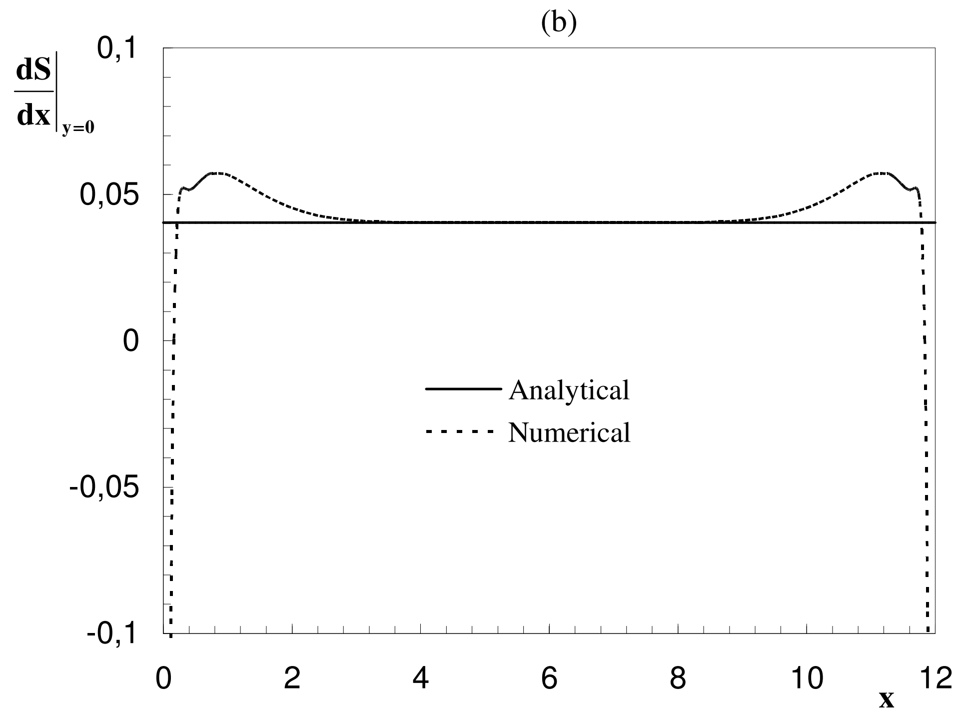

Fig. 3 (Er-Raki et al.)

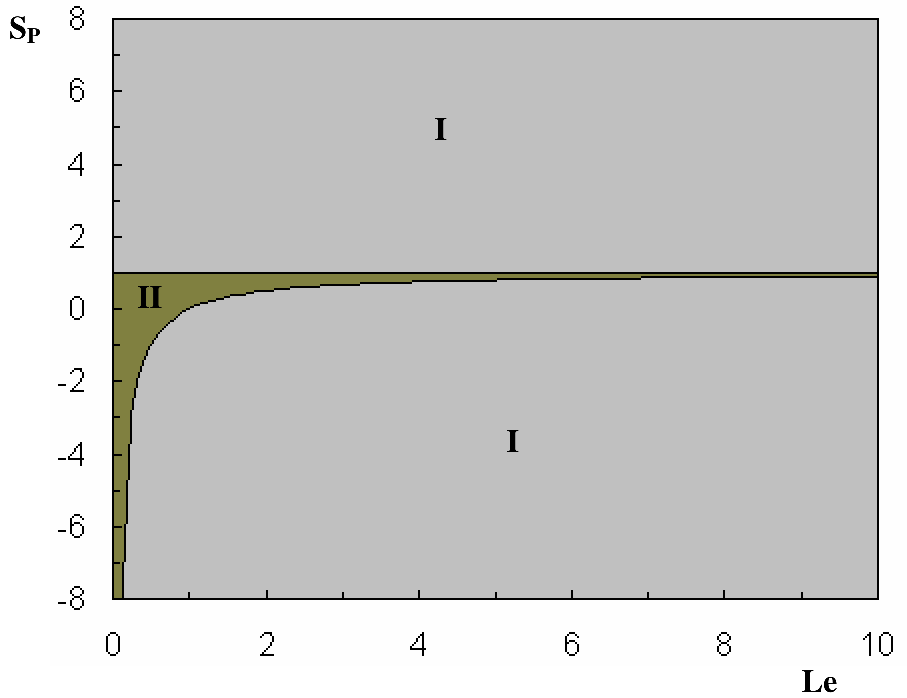

Fig. 4 (Er-Raki et al.)

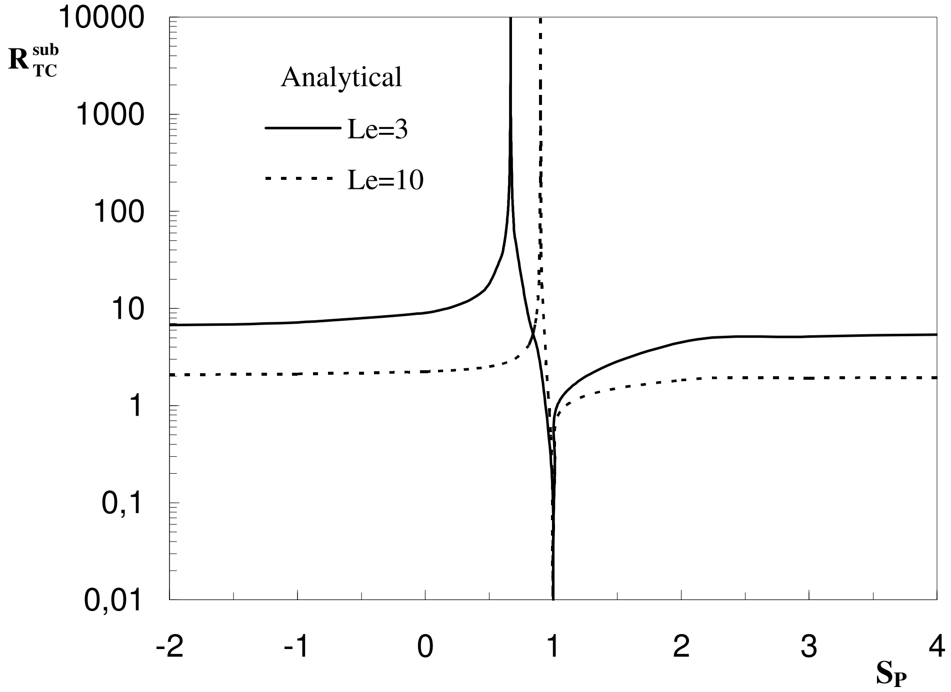

Fig. 5 (Er-Raki et al.)

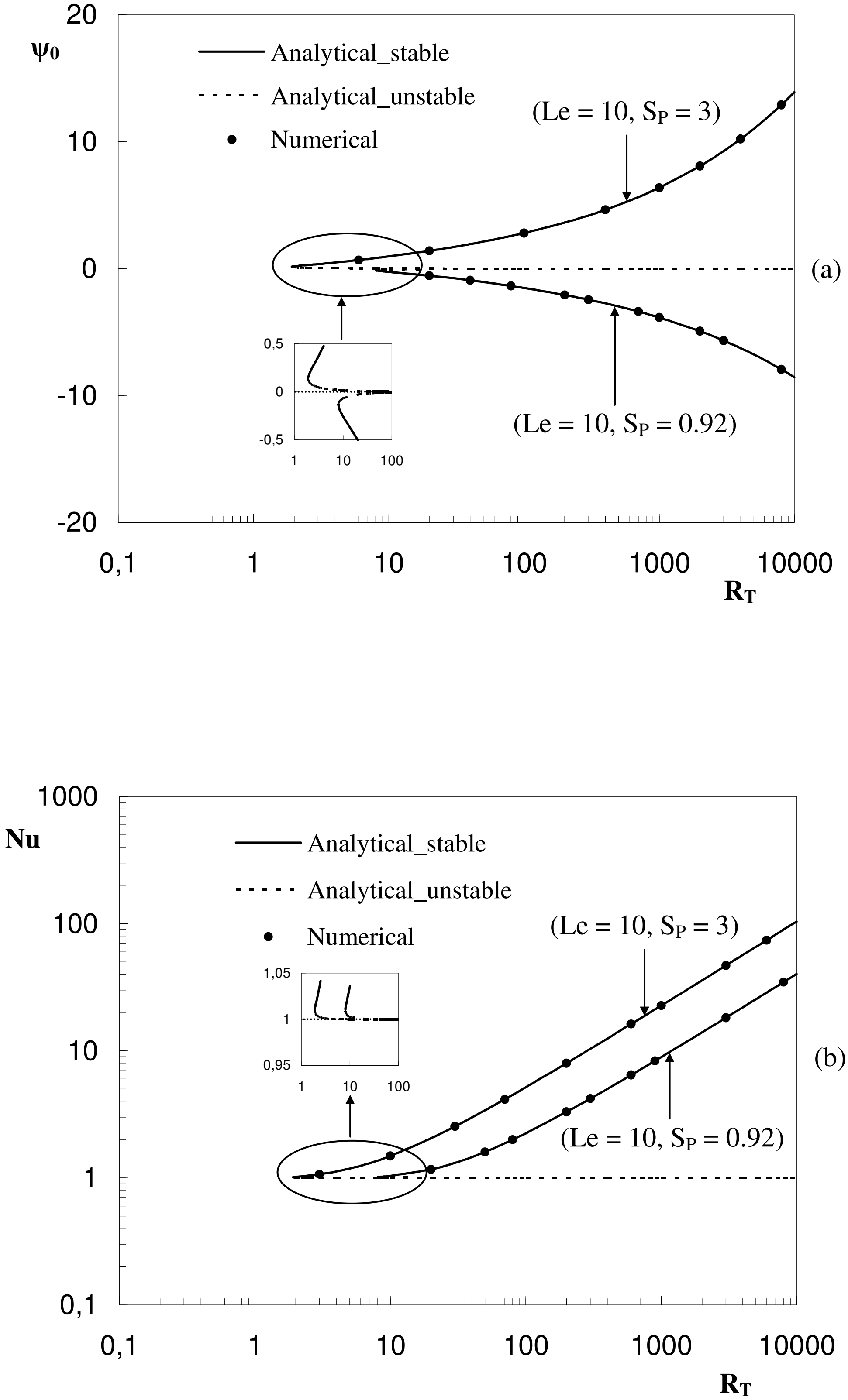

Fig. 6 (Er-Raki et al.)

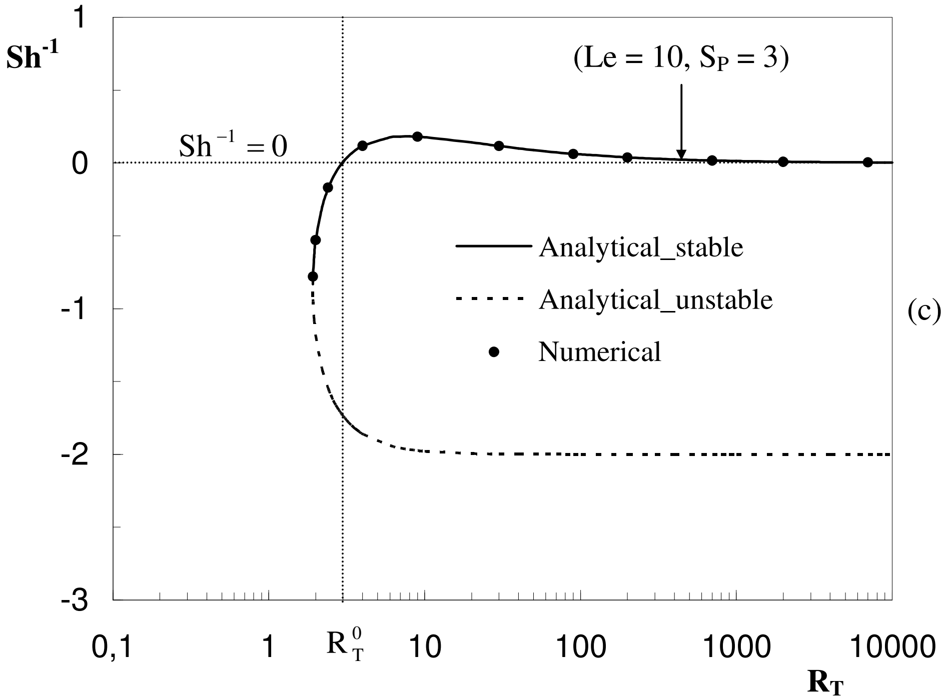

(c)

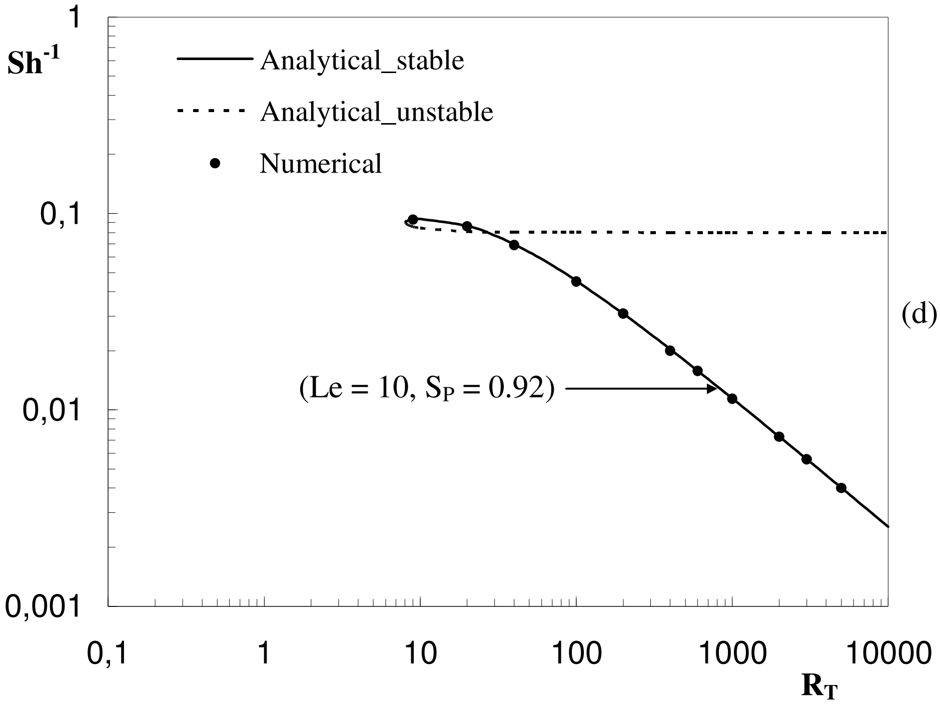

(d)

Fig. 6- continued (Er-Raki et al.)

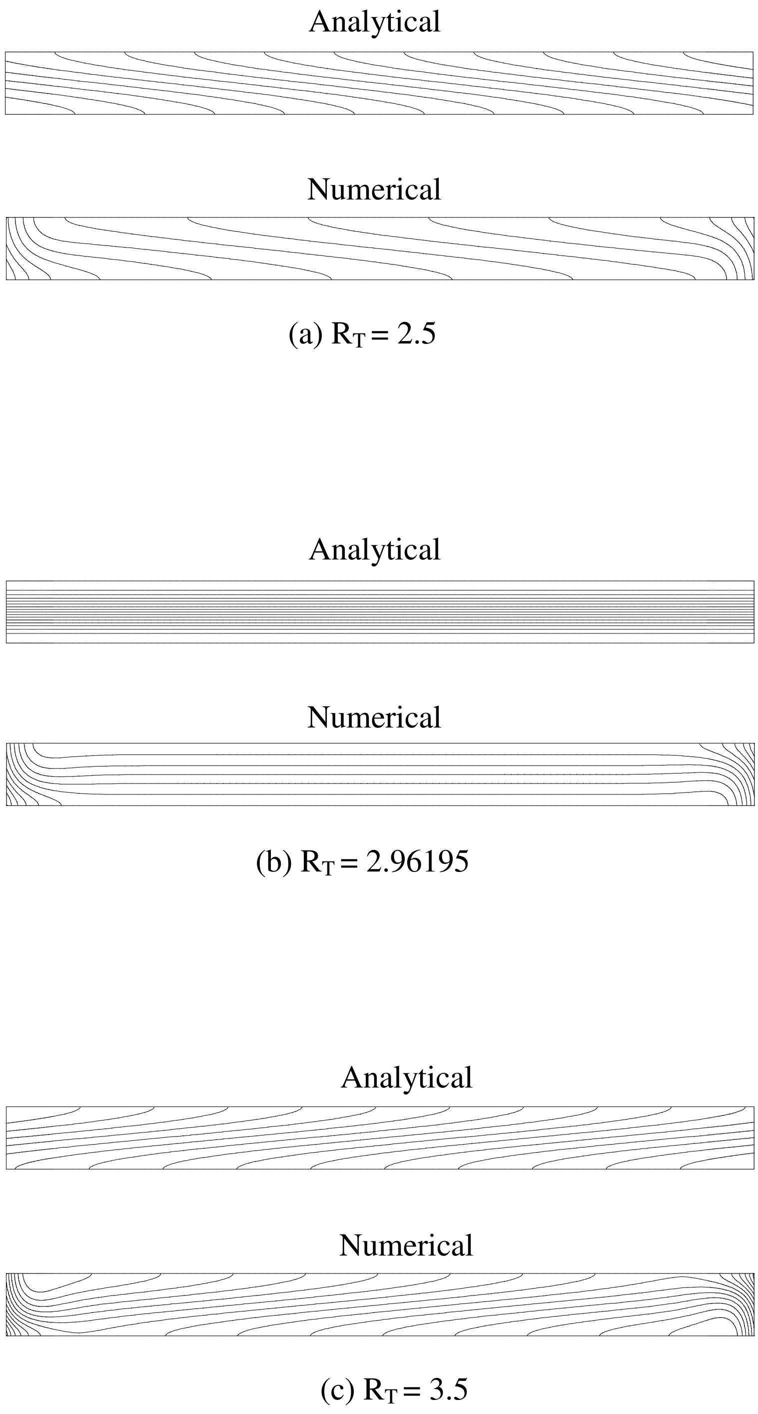

Fig. 7 (Er-Raki et al.)

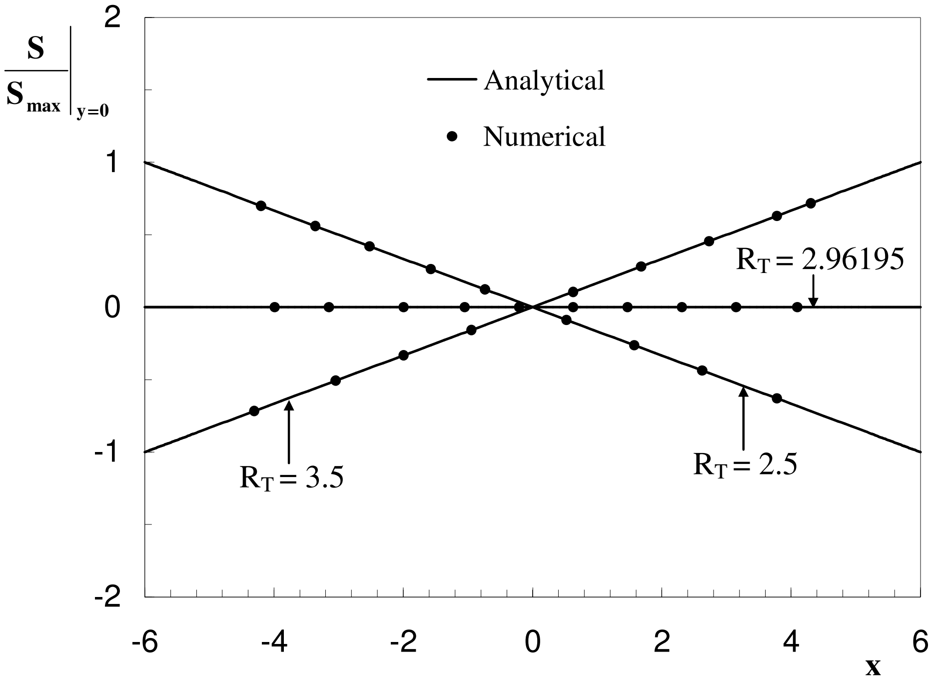

(d)

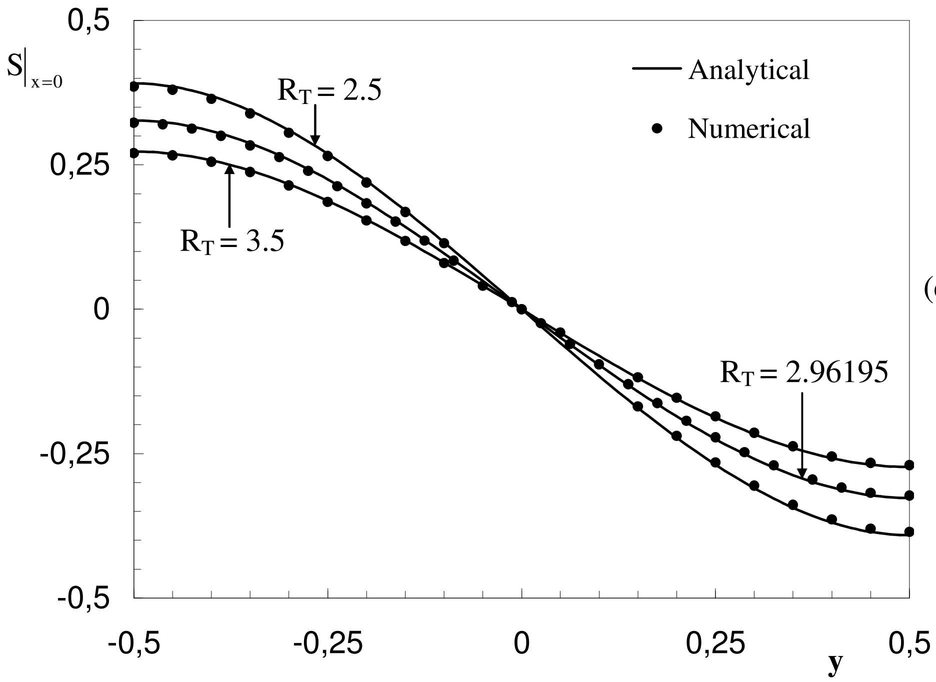

(e)

Fig. 7-continued (Er-Raki et al.)

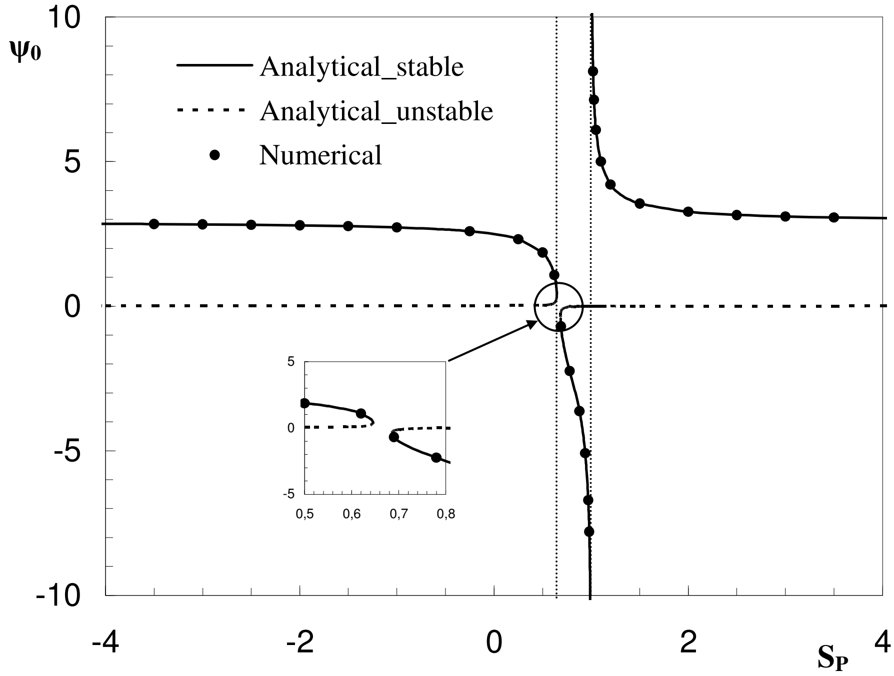

(a)

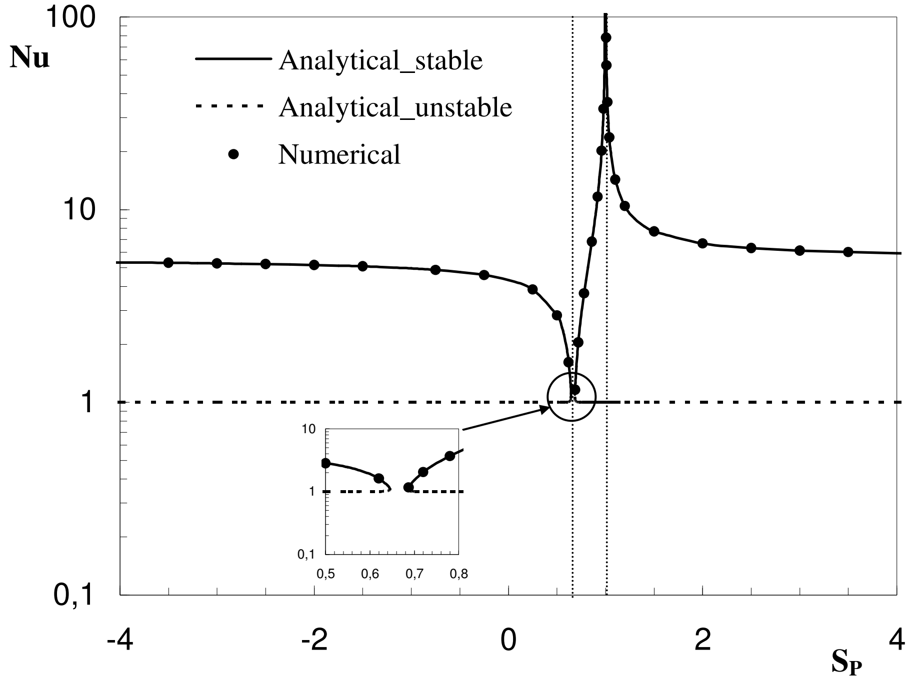

(b)

Fig. 8 (Er-Raki et al.)

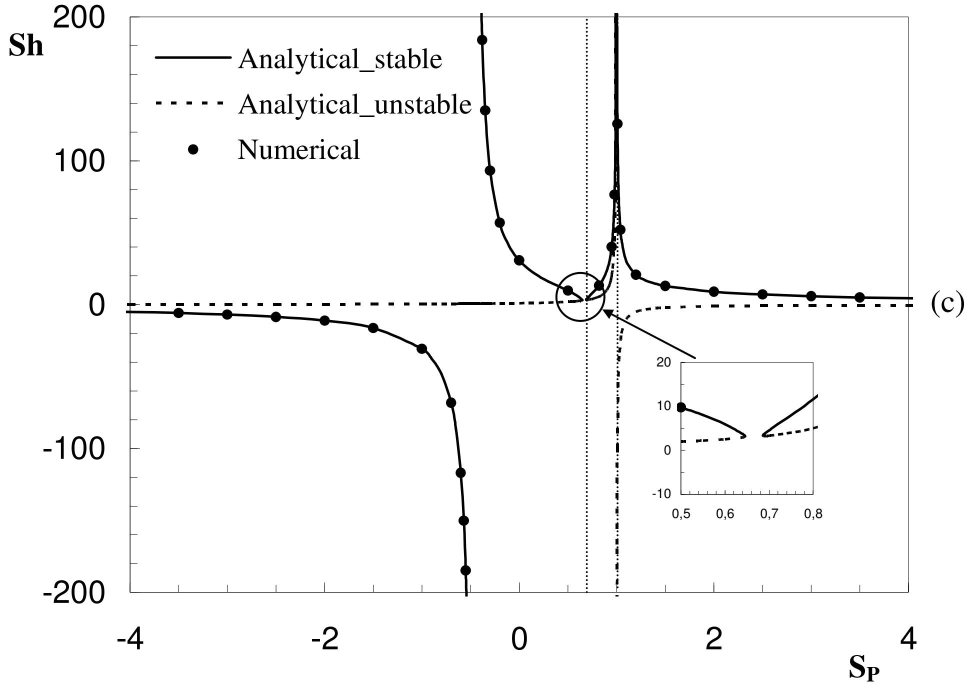

Fig. 8-continued (Er-Raki et al.)